

Interruption of Lung Cancer Cell Migration and Proliferation by Fungal Immunomodulatory Protein FIP-fve from *Flammulina velutipes*

Yu-Chi Chang,[†] Yi-Min Hsiao,[‡] Ming-Fang Wu,^{§,||} Chu-Chyn Ou,[⊥] Yu-Wen Lin,[†] Ko-Huang Lue,^{*,||,#} and Jiunn-Liang Ko^{*,†,‡,#}

[†]Institute of Medicine, Chung Shan Medical University, No. 110, Sec. 1, Chien-Kuo N. Road, Taichung 40203, Taiwan

[‡]Department of Medical Laboratory Science and Biotechnology, Central Taiwan University of Science and Technology, Taichung 40601, Taiwan

[§]Department of Medical Oncology and Chest Medicine, Chung-Shan Medical University Hospital, Taichung 40203, Taiwan

^{||}School of Medicine, Chung Shan Medical University, Taichung 40203, Taiwan

[⊥]School of Nutrition, Chung Shan Medical University, Taichung, 40203, Taiwan

[#]Division of Allergy, Department of Pediatrics, Chung-Shan Medical University Hospital, Taichung 40203, Taiwan

ABSTRACT: FIP-fve is an immunomodulatory protein isolated from *Flammulina velutipes* that possesses anti-inflammatory and immunomodulatory activities. However, little is known about its anticancer effects. It is suppressed cell proliferation of A549 lung cancer cells on MTT assay following 48 h treatment of FIP-fve. FIP-fve treatment also resulted in cell cycle arrest but not apoptosis on flow cytometry. This immunomodulatory protein was observed to increase p53 expression, as well as the expression of its downstream gene p21, on Western blot. FIP-fve inhibited migration of A549 cells on wound healing assay and decreased filopodia fiber formation on labeling with Texas Red-X phalloidin. To confirm the effect of FIP-fve on the role of Rac1 in filopodia formation, we investigated the activity of Rac1 in A549 cells following FIP-fve treatment. FIP-fve inhibited EGF-induced activation of Rac1. We demonstrated that FIP-fve decreases RACGAP1 mRNA and protein levels on RT-PCR and Western blot. In addition, the reporter activity of RACGAP1 was reduced by FIP-fve on RacGAP1 promoter assay. Silencing of RacGAP1 decreased cell migration, and overexpression of RacGAP1 increased cell migration in A549 cells. In conclusion, FIP-fve inhibits lung cancer cell migration via RacGAP1 and suppresses the proliferation of A549 via p53 activation pathway.

KEYWORDS: FIP-fve, lung cancer, A549 cells, metastasis, proliferation, RacGAP1

■ INTRODUCTION

Lung cancer is one of the most common malignancies in the world and is a leading cause of cancer-related death in many countries. Non-small cell lung cancer (NSCLC) accounts for approximately 85% of all lung cancers. Despite advanced therapy, NSCLC still has poor clinical response. To improve the clinical responses and outcomes of NSCLC patients, it needs to develop novel drugs and strategies for preventing proliferation and metastasis of cancer cells.

Cell migration is a complex process involving the reorganization of actin cytoskeleton that correlates with cancer prognosis. Rho GTPases are key factors in cell proliferation, polarity, cytoskeletal remodeling, and migration. Abnormal function of their regulators may result in cell transformation.² Rho GTPases, including Rac, Cdc42, and Rho, are essential factors for facilitating cell migration. It has been reported that δ -catenin affects cytoskeletal assembly and promotes cell migration via regulation of the activity of small GTPases. NSCLC patients with coexpression of δ -catenin and small GTPases have a shorter survival time than those without coexpression.³ The activity of Rho GTPases is down-regulated in nonmalignant mammary epithelial cells (MECs) on three-dimensional culture, with particular suppression of Rac1 and Cdc42.⁴ Rac signaling also regulates cellular functions in the initiation and

maintenance of hematopoietic malignancies.⁵ Increasing Rac activity not only induces autonomous protrusion but also leads to retraction of side and back cells. This results in net cluster polarization and movement in the direction of highest Rac activity.⁶ Deleted in liver cancer-1 (DLC1) is a tumor suppressor gene that encodes a protein with strong RhoGAP (GTPase activating protein) activity and weak Cdc42GAP activity. It is inactivated in various human malignancies.⁷

Fungal immunomodulatory protein (FIP-fve) has been isolated and purified from the edible golden needle mushroom (*Flammulina velutipes*).⁸ It is a glycoprotein in which a potential N-glycosylation site is present at position 54.⁹ FIP-fve exhibits hemagglutinating activity toward four types of human red blood cells. In BALB/c mice sensitized by subcutaneous or intraperitoneal injection of BSA, treatment with six or seven biweekly injections of FIP-fve resulted in no anaphylactic reaction.⁸ FIP-fve has also been found to stimulate the production of IFN- γ in human peripheral blood mononuclear cells (PBMCs).¹⁰ In a previous study, FIP-fve stimulated IFN- γ production via the

Received: July 11, 2013

Revised: October 4, 2013

Accepted: November 18, 2013

Published: November 18, 2013

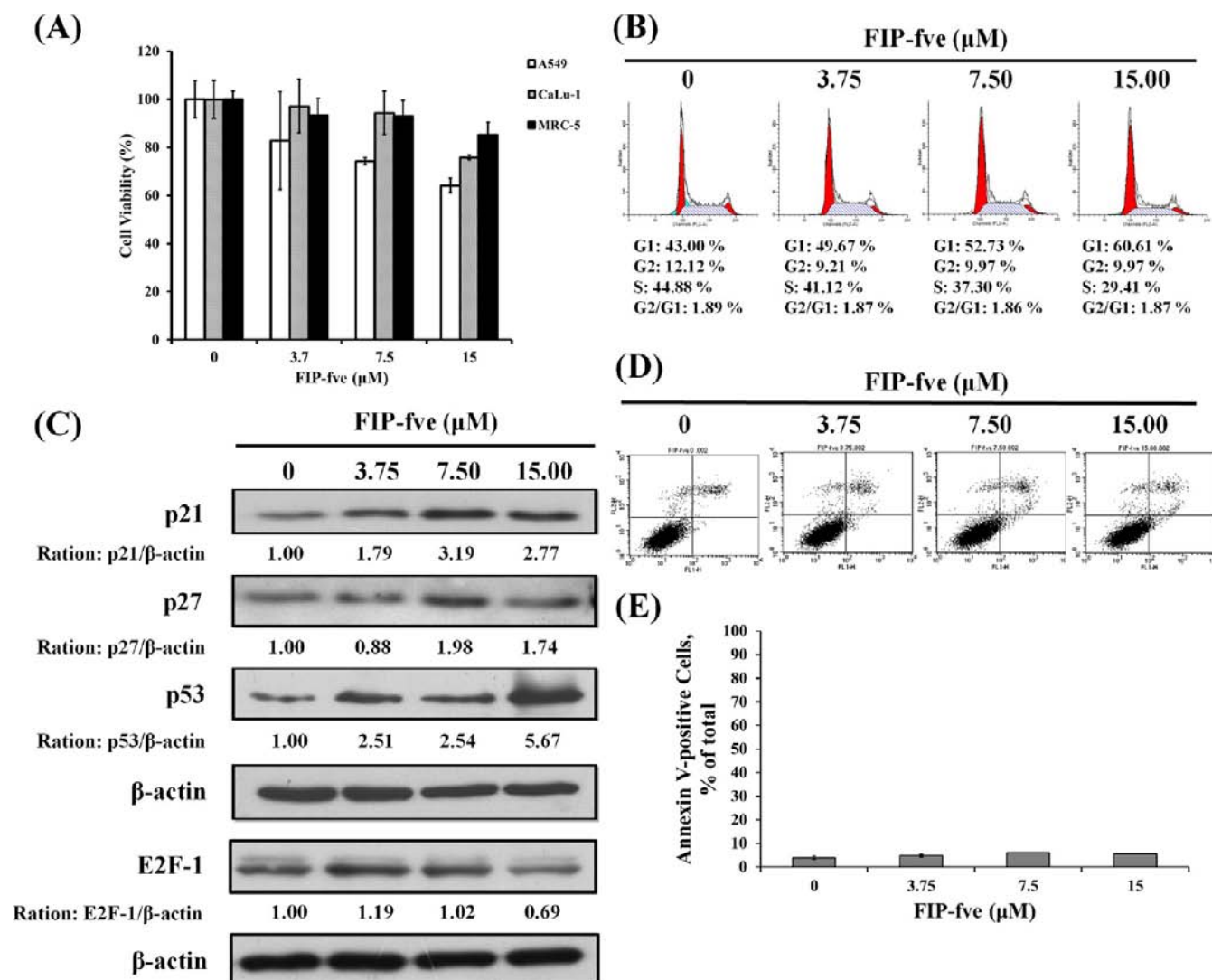


Figure 1. Effect of FIP-fve on cell viability. (A) A549, CaLu-1, and MRC-5 cells (5×10^3 /well of 96-well plate) were treated with varying concentrations of FIP-fve (0, 3.75, 7.50, and 15.00 μM) for 48 h, followed by MTT assay to estimate cell viability. (B) A549 cells (3×10^5 /6 cm dish) were incubated with FIP-fve (0, 3.75, 7.50, and 15.00 μM) for 48 h. Cell cycle phases were analyzed using a fluorescence activated cell sorter with ModFIT 3.0 software. (C) A549 cells (5×10^5 /6 cm dish) were untreated or treated with 3.75, 7.50, and 15.00 μM FIP-fve for 48 h. The total cellular lysates were analyzed using Western blot for the expressions of p21, p27, p53, E2F-1, and β -actin proteins. (D) A549 (3×10^5 /6 cm dish) cells were treated with various concentrations of FIP-fve (0, 3.75, 7.50, and 15.00 μM) for 48 h. The induction of apoptosis was determined by flow cytometric analysis of Annexin V-FITC and PI-staining. (E) phase percentages for upper right quadrant and lower right quadrant are depicted on bar graph.

modulation of Ca^{2+} release.¹¹ Tumor growth suppression is associated with an increase in polyfunctional T cells that secrete multiple effector cytokines, such as $\text{IFN-}\gamma$, IL-17, and IL-2. In mice deficient in IL-17 or deprived of $\text{IFN-}\gamma$, therapeutic protection is abolished.¹² $\text{IFN-}\gamma$ pretreatment and silencing of antiapoptotic protein XIAP may lead to a rise in TRAIL-induced apoptosis and to caspase-8 up-regulation.¹³

In this study, RACGAP1 served as a novel therapeutic target in lung cancer. FIP-fve may be a potential anticancer agent able to inhibit A549 migration via decreasing RACGAP1 expression and to suppress proliferation via p53 activation pathway.

MATERIALS AND METHODS

Purification of Fungal Immunomodulatory Protein FIP-fve.

FIP-fve was purified as previously described.⁸ In brief, the fruit bodies of *F. velutipes* (300 g) were homogenized with ice-cold 5% acetic acid in the presence of 0.05 M 2-mercaptoethanol. Soluble proteins in the

supernatant were precipitated by the addition of ammonium sulfate to 80% saturation. The precipitate was collected and then dialyzed against 10 mM sodium acetate pH 5.2 at 4 °C for 36 h with three changes in dialysis solution. The dialysate was applied to a CM-52 column (2 cm \times 5 cm), which was previously equilibrated with 10 mM sodium acetate, pH 5.2. The column was first washed with 200 mL of equilibration buffer and then eluted with 200 mL of 0–0.5 M NaCl in 10 mM sodium acetate, pH 5.2. The active fractions were collected with 80 mg (300 μM) of purified FIP-fve.

Cell Culture. A549 human lung adenocarcinoma cells were obtained from the American Type Culture Collection. Cells were maintained at 37 °C in a 5% CO_2 humidified atmosphere in Dulbecco's Modified Eagle's Medium (DMEM) (GIBCO, Rockville, MD) containing 10% fetal bovine serum (FBS; Life Technologies, Inc., Rockville, MD), 100 units/mL penicillin, and 100 $\mu\text{g}/\text{mL}$ streptomycin (Life Technologies, Inc.).

MTT Assay. Following FIP-fve treatment for 48 h, cell viabilities of the A549, CaLu-1, and MRC-5 cells were analyzed on MTT assay. The complete protocol for MTT assay has been described elsewhere.¹⁴

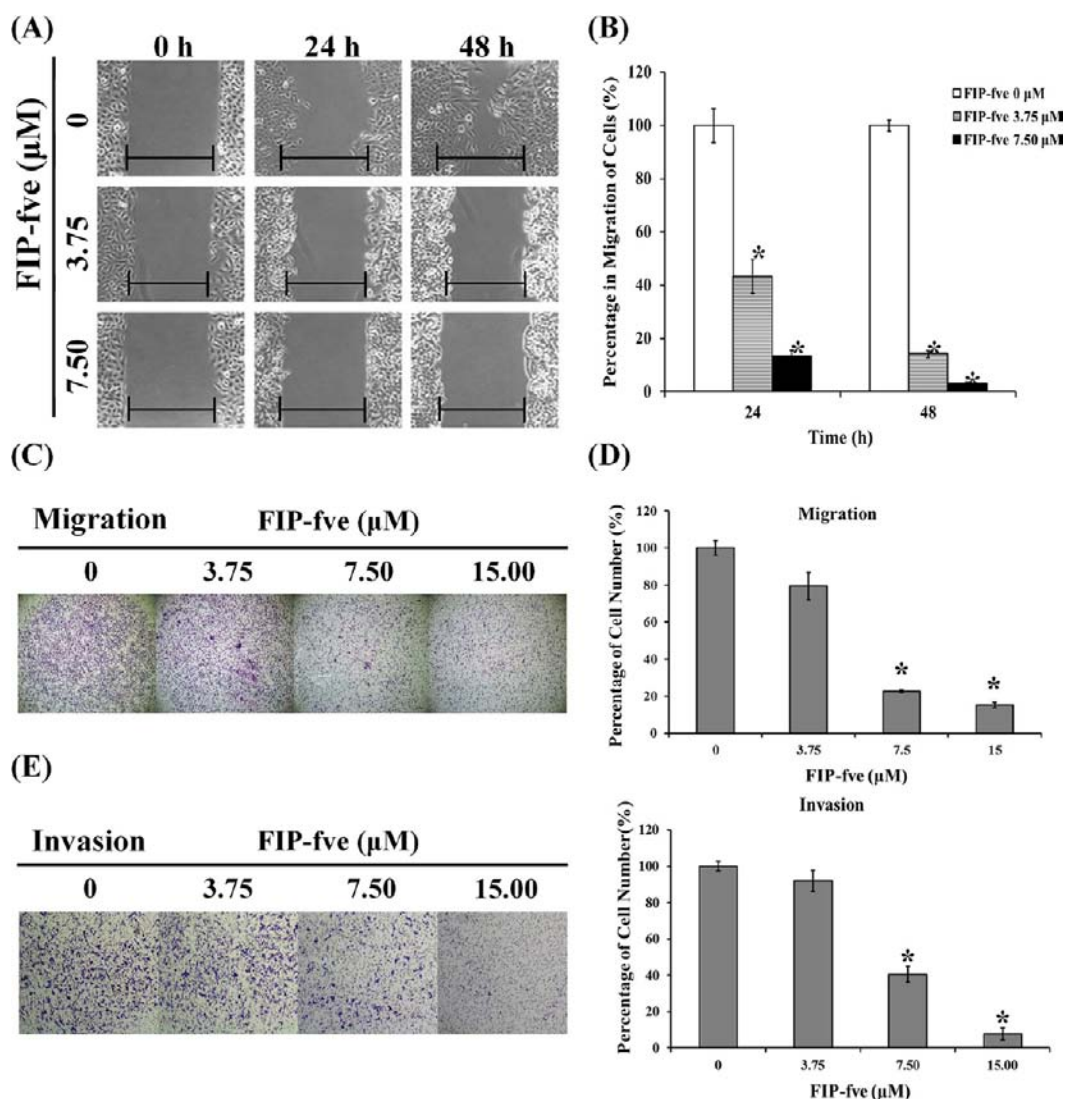


Figure 2. Effect of FIP-fve on cell metastasis. (A,B) A549 cells were seeded onto culture insert overnight (2×10^4 /well), then treated with FIP-fve. After incubation for 24 and 48 h, cell migration (wound healing) was monitored by microscopy. A549 lung cancer cells (2×10^5) treated with FIP-fve (0, 3.75, 7.50, and 15.00 μM) were allowed to migrate to 10% FBS-DMEM for 8 or 24 h. The migrated (C,D) and invaded (E,F) cells were quantified by counting. Cells were fixed, stained, and counted as described in the text. The data represent mean \pm SD.

Cell Cycle Analysis. The cell cycle distribution was analyzed by flow cytometry. The complete protocol for flow cytometry has been previously described.¹⁵

Annexin V-FITC/PI Staining. Percentage of apoptosis was measured using the FITC Annexin V apoptosis detection kit I (556547, BD Pharmingen) with flow cytometry. Staining was performed according to the manufacturer's protocol. Then 1×10^6 cells per sample were analyzed using a flow cytometer (FACScan, Becton-Dickinson, San Jose, CA) with Cellquest software.

Wound Healing Assay. A549 cells were seeded onto culture insert (Ibidi, München, Germany). Cells were plated onto 24-well plates at 2×10^4 cells/well to nearly confluent cell monolayer. The monolayer was then washed twice with phosphate-buffered saline (PBS) to remove debris or detached cells following treatment with differing concentrations of FIP-fve (0, 3.75, 7.50, and 15.00 μM). Following incubation for 24 and 48 h, the cells were photographed under a light microscope (magnification, $\times 200$).

Reporter Gene Assay. Reporter plasmid pGL3-RacGAP1-luc was constructed by excising the *KpnI/HindIII* fragment from the amplified RacGAP1 promoter DNA and subcloning it into pGL3-Basic (Promega). Reporter plasmid pGL3-RacGAP1-luc (77783–79123) was constructed according to accession no. AC025154.31 (Genbank).

The RacGAP1 promoter was cloned upstream of the firefly luciferase reporter in the pGL3-Basic vector (Promega, Madison, WI, USA). Briefly, a -1240 to $+99$ segment of the 5'-flanking region of the human RacGAP1 gene was amplified by PCR using specific primers with restriction enzyme site from the human RacGAP1 gene: 5'-GGGGTACCCTGCGTGACAGAGTAAGACCCT (forward/*KpnI*) and 5'-GGAAGCTTCTCACTTCAGTCAGCCTGGCCCC (reverse/*HindIII*). A549 cells were seeded onto 24-well plate and incubated for 16 h. Then RacGAP1 promoter-luciferase construct and β -galactosidase expression plasmid were cotransfected as previously described.¹⁶ After 24h transfection, cells were treated with FIP-fve for 48 h followed by collection and analysis on a Luciferase Assay System (Promega, Madison, WI, USA). Finally, luciferase activities were standardized for β -galactosidase activity.

Actin Staining. A549 cells were fixed with 3.7% paraformaldehyde-PBS solution for 10 min. After two additional washes with PBS, cells were permeabilized with 0.1% Triton X-100 in PBS. Texas Red-X phalloidin (2 units/ml) and Alexa Fluor 488 DNase I conjugate (9 $\mu\text{g}/\text{mL}$) in 1% bovine serum albumin and 0.025% saponin-PBS were used to localize filamentous actin (F-actin) and DNase I staining (G-actin) for 1 h. After three washes with PBS, coverslips were mounted onto a microscope slide with Prolong Gold antifade reagent

with DAPI (Life Technologies). Cell imaging was performed with a confocal laser scanning microscope.

RT-PCR and Real-Time PCR. The primer sequences used for PCR amplification were: RacGAP1 sense 5'-5'ACAGGGACACATTAGCTTTCTC-3' and antisense 5'-CTGACTTCACTTGAGCATTGAG-3'; lipocalin 2 sense 5'-GAGTTACCCTGGATTAACGA-3' and antisense 5'-CTCCTTTAGTTCGGAAGTCA-3';¹⁶ β -actin sense 5'-CAGGGAGTGATGGTGGGCA-3' and antisense 5'-CAAACATCATCTGGT CATCTTCTC-3';¹¹ PAI-1 sense 5'-GGATCCGTGCCG-GACCACAAAGAGGAA-3' and antisense 5'-GGATCCAGC-CACTGGAAGGCAACATG-3'; NM23 sense 5'-TGCTGCGAAC-CACGTGGGTCCCGG-3' and antisense 5'-TCATTATAGATC-CAGTTCTGAGCA-3'; and MMP2 sense 5'-GGCCCTGT-CACTCCTGAGAT-3' and antisense 5'-GGCATCCAGGTTATC-GGGGA-3'. The detailed protocols for RNA isolation and RT-PCR have been previously described.¹⁷ By using the ABI PRISM 7000 real-time PCR system and a TaqMan gene expression probe (Applied Biosystems, Foster City, CA), real-time PCR analyses of NM23 (Hs00264824_m1), MMP2 (Hs00234422_m1), and GAPDH (Hs99999905_m1) gene expression levels were carried out by using assays-on-gene expression products. Concentrations of synthesized primers and probes were optimized for each assay, then, real-time PCR was performed in triplicate in a 10 μ L reaction volume. The PCR reaction included 50 $^{\circ}$ C 2 min and 95 $^{\circ}$ C 10 min, followed by 45 $^{\circ}$ C cycles, each consisting of 95 $^{\circ}$ C 15 s and 60 1 min. Quantitative values were obtained from the threshold PCR cycle number (CT), where the increase in signal associated with an exponential growth of PCR product became detectable. The relative mRNA levels of nm23 and MMP2 in each sample were normalized to its GAPDH content. Real-time PCR quantification of NM23 and MMP2 was carried out by using TaqMan analysis. All values are normalized to the level of GAPDH and are the averages of three independent readings.

Rac1 and Cdc42 Activity Assay. Active Rac1 and Cdc42 were detected on pull-down assay. The complete protocol has been described in a previous study.¹⁸ In short, serum-starved A549 cells were collected in 800 μ L of ice-cold lysis buffer following stimulation for 3 min with EGF. Lysates were centrifuged and supernatant was removed to measure protein content using Protein Assay Kit (Bio-Rad, Hercules, CA) at 5 μ L per sample. Then 20 μ L of lysates were used to determine total Rac1 and Cdc42 of total lysate, with the remainder used for pull-down assay. Equal amounts of protein lysates were then mixed with 15 μ g of GST-PAK-PBD-beads (Pierce, Rockford, IL, USA). Samples for total Rac1 and Cdc42 in total lysate and pelleted beads were diluted in Laemmli sample-buffer and boiled. SDS-PAGE (12% gel) was performed to separate the proteins. After transfer to polyvinylidene fluoride membranes (PALL, Pensacola, FL), the transferred membranes were blocked with 3% bovine serum albumin, followed by incubation with Rac1 antibody overnight. Binding of the antibody was visualized using antimouse IgG HRP conjugated antibody and chemiluminescence substrate (Perkin-Elmer Life Sciences). Equal loading was confirmed by reprobings of membranes with anti- β -actin antibody.

Western Blot Analysis. Western blot was performed to investigate the presence of particular proteins or phosphorylated forms of proteins. Cells were washed with ice-cold phosphate buffered saline and lysed in RIPA with Complete and Phosphostop buffer (Roche). Whole cell lysate were lysed by sonication. Cell lysates were centrifuged 12000 rpm for 10 min. Supernatant was used for Western blot assay. Whole-cell extracts (WCE) were prepared on ice, quantified using Bio-Rad protein assay (Bio-Rad, Hercules, CA), and resolved by SDS-PAGE electrophoresis, followed by immunoblot analysis. Proteins were immunodetected using anti-p21 (no. 2946, Cell Signaling), anti-p27 (no. 06-445, Upstate), anti-p53 (M 7001, DakoCytomation), anti-E2F-1 (no. 05-379sp, Millipore), anti-RacGAP1 (GTX113320, Gene-Tex, Inc.), and anti- β -actin (AC-40, Sigma, St. Louis, MO) diluted in PBS containing 0.5% Tween and 5% nonfat dry milk. The membranes were further incubated for 1 h with horseradish peroxidase-labeled antirabbit or antimouse IgG (Cell Signaling Technology, Beverly, MA, USA) or blocking solution. ECL Western blotting detection reagents (Amersham Milan, Italy) were used to visualize specific hybridization

signals. Blots were then developed with an enhanced luminol chemiluminescence (ECL) reagent (NEN, Boston, MA).

Cell Invasion Assay. Cell invasion assays were performed using modified Boyden chambers (Transwell; Costar, Cambridge, MA).¹⁸ To the lower chamber was added 10% FBS-DMEM, while the membrane of the upper chamber was coated with Matrigel (0.3 mg/mL; BD Biosciences Discovery Labware) for 3 h. A549 cells were pretreated with FIP-fve (0, 3.75, 7.50, 15.00 μ M) for 48 h and collected, followed by resuspension at 2×10^5 cells/well in 0.5% FBS-DMEM. After 24 h incubation, the cells on the membrane were fixed with methanol and stained with 20% Giemsa solution (Merck). The cells were counted under a light microscope (magnification, 100 \times). The experiments were performed in triplicate.

RESULTS

FIP-fve Reduces Cell Viability of A549 Lung Cancer Cells through Induction of G1 Arrest. To assess the effects of FIP-fve on lung cancer cell viability, A549 cells were treated with FIP-fve for 48 h and analyzed on MTT assay. It has been reported that P53 and p53-associated factors, p21 and p27, prevent the emergence of cancer cells by initiating cell cycle arrest¹⁹ and releasing the transcriptional factor E2F-1 to initiate cell cycle progression to S phase.²⁰ The results of this study showed that FIP-fve decreases lung cancer cell viability in a concentration dependent manner (Figure 1A). Compared with untreated cells, cell viability decreased to 60% at 15.00 μ M. Calu-1 without P53 is more resistant than A549 cells with

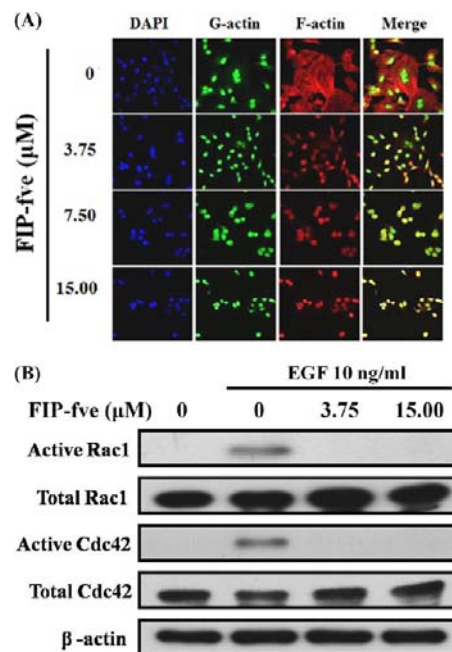


Figure 3. Effect of FIP-fve on cell cytoskeleton. (A) A549 cells (1×10^4 /well) were seeded onto 24-well plate with coverslip and pretreated with varying concentrations of FIP-fve (0, 3.75, 7.50, and 15.00 μ M) for 24 h. They were then stained with Texas Red-X phalloidin and Alexa Fluor 488 DNase I conjugate to detect F-actin (red) and G-actin (green). F-Actin labeling with Texas Red-X phalloidin revealed that A549 cells exhibit numerous filopodia fibers, whereas FIP-fve-treated cells exhibit fewer filopodia fibers. (B) A549 cells (2×10^6 /10 cm dish) were treated with varying doses of FIP-fve (3.75, 15.00 μ M) for 24 h before being stimulated with 10 ng/mL EGF for 3 min. GTP-bound Rac1 was pulled down using the GST-PBD fusion protein of PAK1 immobilized on glutathione beads, and total Rac1 was detected with anti-Rac1 and antibodies.

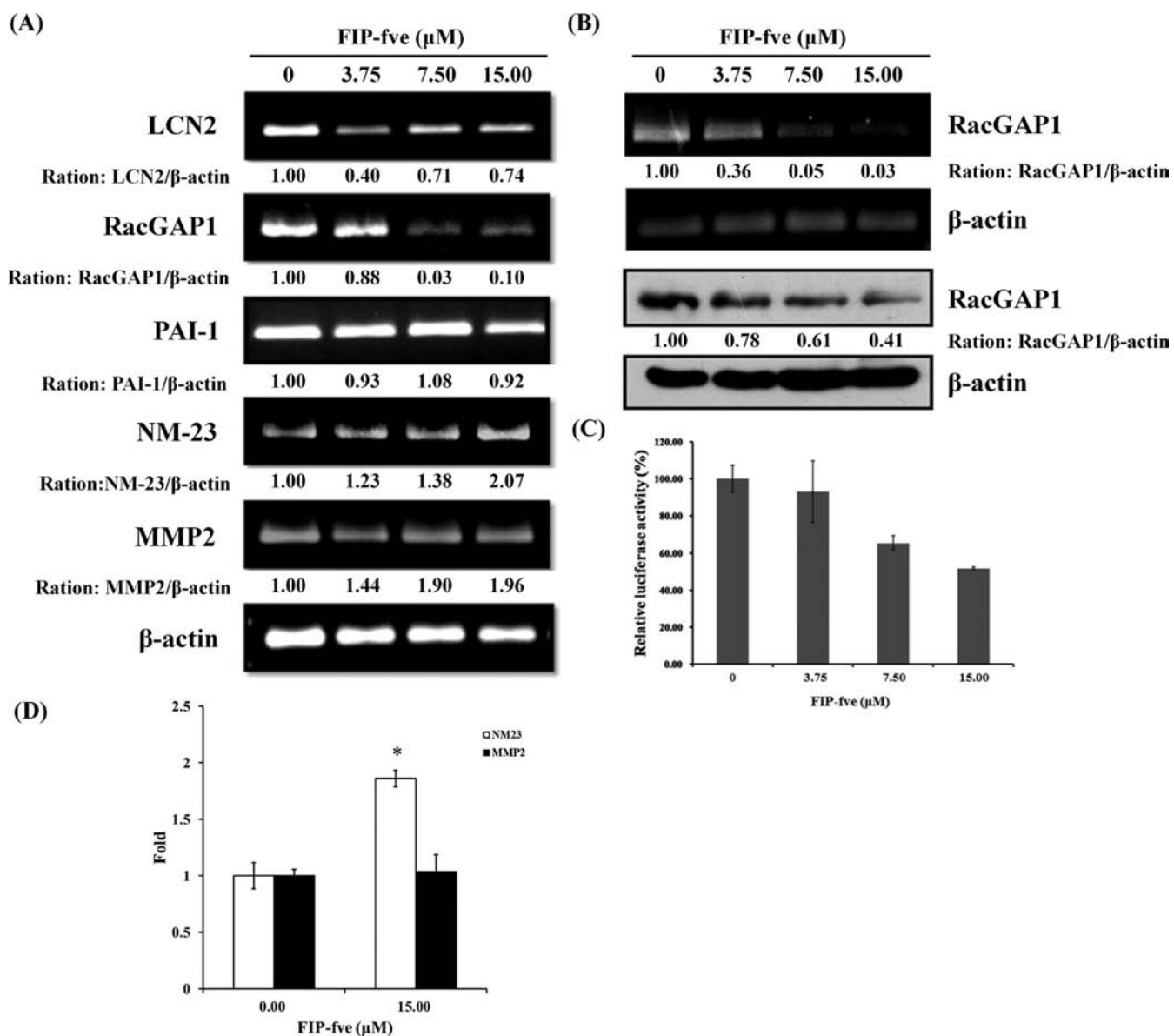


Figure 4. Effect of FIP-fve on LCN2, RacGAP1, PAI-1, nm-23, and MMP2 mRNA expressions of A549 cells. (A) A549 cells ($5 \times 10^5/6$ cm dish) were untreated or treated with 3.75, 7.50, or 15.00 μM FIP-fve for 48 h. The total RNA was analyzed using RT-PCR for LCN2, RacGAP1, PAI-1, nm-23, MMP2, and β -actin mRNA expressions. (B) Total cellular RNA and protein from A549 cells ($5 \times 10^5/6$ cm dish), untreated or treated with 3.75, 7.50, or 15.00 μM FIP-fve for 48 h, were analyzed using RT-PCR (upper photo) or Western blot (lower photo) for RacGAP1 and β -actin expressions. (C) A549 cells were plated onto 24 wells (5×10^4 /well) and incubated at 37 $^\circ\text{C}$. At 70–80% confluency, 0.8 μg of pGL3-RacGAP1-luc promoter containing pGL3 vector, and 0.2 μg of β -galactosidase vector were transfected using jetPEITM reagent. After 48 h, treatment was carried out at varying concentrations of FIP-fve. After 48 h incubation, cells were lysed and luciferase activity was measured using a luminometer. β -Galactosidase activity was measured using *o*-nitro-phenyl β -galactopyranoside as a substrate. (D) Real-time PCR quantification of NM23 and MMP2 was carried out by using TaqMan analysis. All values are normalized to the level of GAPDH and are the averages of three independent readings.

wild-type P53 under FIP-fve treatment in the MTT assay. They are low cytotoxicity for normal lung fibroblast MRC-5 cells (Figure 1A). Flow cytometry was used to determine whether A549 cells treated with FIP-fve undergo cell cycle arrest or increase in apoptosis. FIP-fve treatment resulted in an increase in the G1 population after 48 h treatment (Figure 1B). We detected p21, p27, p53, and E2F-1 proteins using Western blot. After treatment with FIP-fve for 48 h, p21, p27, and p53 increased and E2F-1 decreased (Figure 1C). Flow cytometric analysis of Annexin V-FITC and PI-staining were performed to detect apoptotic cells. Compared with untreated cells, there was no significant induction of apoptosis following treatment with FIP-fve at various concentrations (Figure 1D). Apoptotic cells

in the LR (Annexin+PI $^-$) and UR (Annexin+PI $^+$) regions were counted, and no more than 7% apoptotic cells were observed (Figure 1E).

Filopodia of Cytoskeleton and Metastasis Decrease Following FIP-fve Treatment in Lung Cancer Cells. To assess the effects of FIP-fve on migration, A549 cells were treated with FIP-fve for 48 h and analyzed on wound healing assay. The results showed that FIP-fve represses A549 cell migration (Figure 2A). At FIP-fve concentrations of 3.75 and 7.50 μM , percentages of migrating cells decreased to 43% and 14% at 24 h and 13% and 3% at 48 h, respectively (Figure 2B). Modified Boyden chamber assay was performed to quantify the migratory and invasive potentials of A549 cells. The results

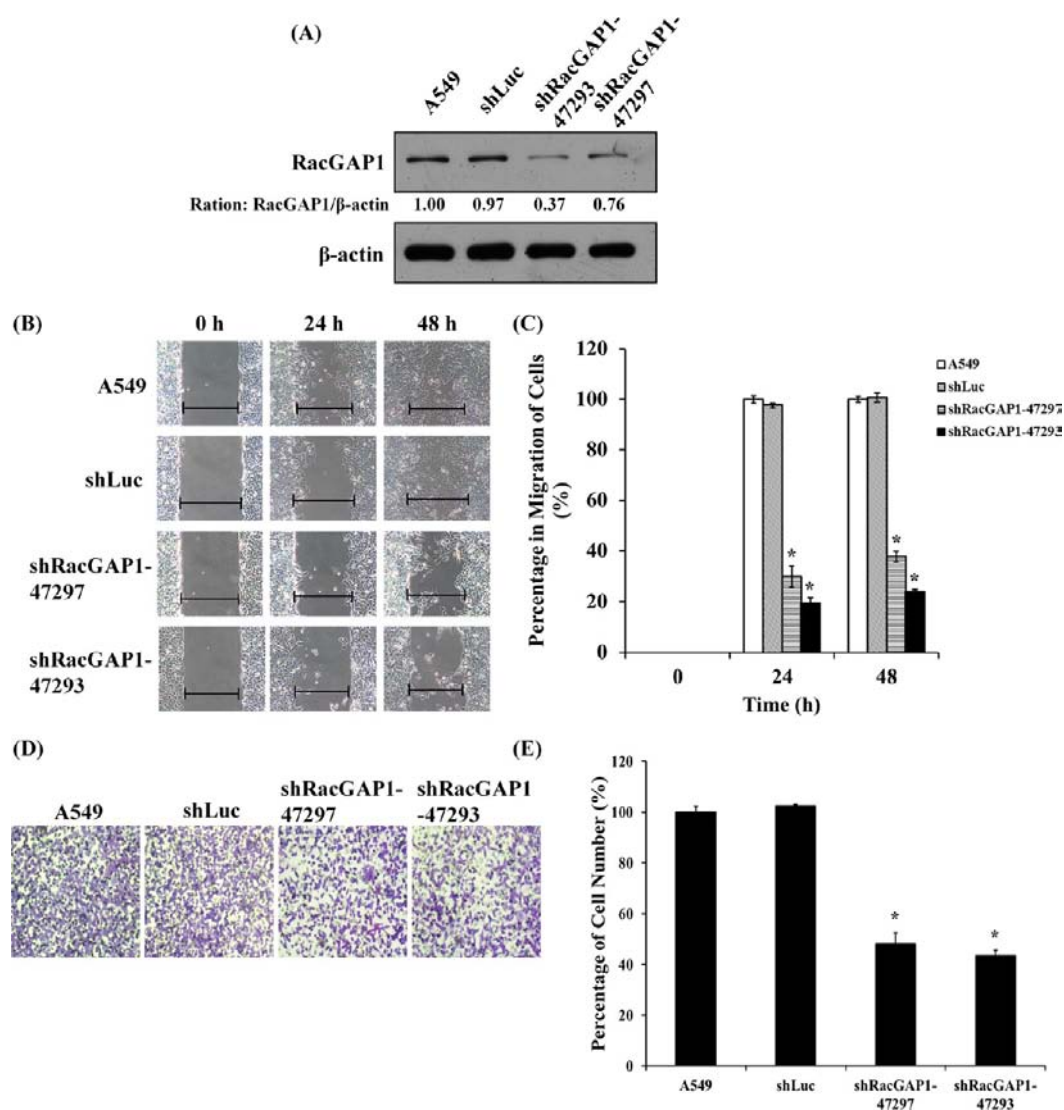


Figure 5. Effect of silencing of RacGAP1 on migration and cell cycle of A549 cells. (A) RacGAP1 gene of A549 cells silenced by lentivirus shRNA system was used to detect RacGAP1 protein expression on Western blot. Lane 1 is parental A549; lane 2 is A549/shLuc as internal control; lane 3 is A549/shRacGAP1-47293; lane 4 is A549/shRacGAP1-47297. (B) A549, A549/shLuc, A549/shRACGAP1-47297, A549/shRACGAP1-47293 cells were seeded onto culture insert overnight (2×10^4 /well, $70 \mu\text{L}$), then treated with FIP-fve (3.75 , $7.50 \mu\text{M}$) for 24 h and 48 h. After incubation for 24 h and 48 h, the extents of cell migration were monitored by microscopy. (C) The percentages of migration of A549, A549/shLuc, A549/shRACGAP1-47297, and A549/shRACGAP1-47293 cells were determined. (D) A549, A549/shLuc, A549/shRACGAP1-47297, and A549/shRACGAP1-47293 cells (4×10^5) were allowed to migrate to 10% FBS-DMEM for 6 h. (E) The migrated cells were quantified by counting. Cells were fixed, stained, and counted as described in the text. The data represent mean \pm SD.

showed that FIP-fve induces dose-dependent decreases in both migration and invasion (Figures 1C,E). Compared to the untreated cells, the proportions of migrating cells were reduced to 79% at $3.75 \mu\text{M}$, 22% at $7.50 \mu\text{M}$, and 15% at $15.00 \mu\text{M}$ (Figure 2D). The proportions of invading cells were reduced to 92% at $3.75 \mu\text{M}$, 40% at $7.50 \mu\text{M}$, and 8% at $15.00 \mu\text{M}$ (Figure 2F). Several studies have shown that actin polymerization, which leads to filopodia assembly and depolymerization, plays a crucial role in cell motility.²¹ To explore the molecular events in response to treatment with FIP-fve, the formations of the F-actin and G-actin cytoskeletons in A549 cells were assessed by staining with Texas Red-X phalloidin and Alexa Fluor 488 DNase I conjugate, respectively. The results showed that FIP-fve suppresses filopodia formation of A549 cells (Figure 3A). On pull down assay, FIP-fve was shown to suppress Rac1 and Cdc42 activation after EGF treatment. Without EGF induction,

Rac1 and Cdc42 were not activated and could not be suppressed. (Figure 3B). Therefore, FIP-fve suppresses, at least in part, the migration of A549 disrupting actin assembly and filopodia formation.

FIP-fve Represses RacGap1 Expression. In previous studies, some genes have been found to be associated with survival or metastatic ability of lung cancer cells, such as lipocalin 2 (LCN2),¹⁶ Rac GTPase-activating protein 1 (RacGAP1),²² plasminogen activator inhibitor type-1 (PAI-1),²³ matrix metalloproteinase (MMP2),²⁴ and human nonmetastatic clone 23 (NM23).¹⁵ We investigated LCN2, RacGAP1, PAI-1, MMP2, and nm-23 mRNA expressions after FIP-fve treatment. RacGAP1 mRNA markedly decreased at 7.50 and $15.00 \mu\text{M}$ (Figure 4A). The RacGAP1 protein expression level detected on Western blot decreased in a dose dependent manner (Figure 4B). To evaluate the effects of FIP-fve on the RacGAP1 promoter, we

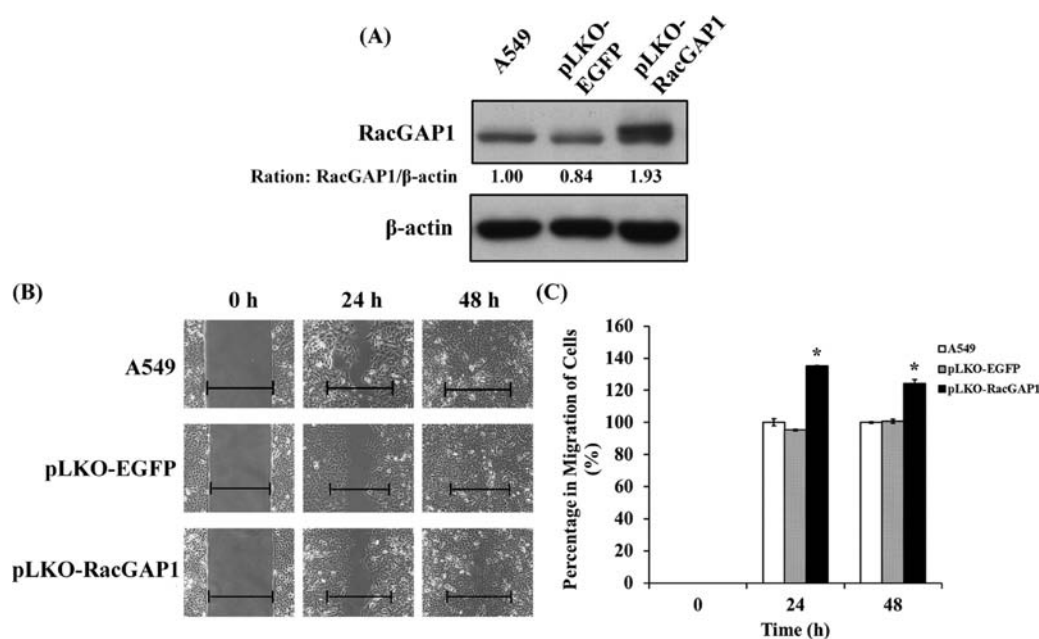


Figure 6. Effect of overexpression of RacGAP1 on migration and cell cycle of A549 cells. (A) RacGAP1 overexpression was confirmed by Western blot. Lane 1 is parental A549; lane 2 is A549/pLKO-EGFP as internal control; lane 3 is A549/pLKO-RacGAP1. (B) A549, A549/pLKO-EGFP, and A549/pLKO-RacGAP1 cells were seeded onto culture insert overnight (2×10^4 /well, $70 \mu\text{L}$). After incubation for 24h and 48 h, the extents of cell migration were monitored by microscopy. (C) The percentages of migration of A549, A549/pLKO-EGFP, and A549/pLKO-RacGAP1 cells were determined.

performed transient transfection with the pGL3-RacGAP1 promoter and analyzed the luciferase activities. As shown in Figure 4C, the luciferase activity of the transfectants treated with FIP-fve (3.75 , 7.50 , $15.00 \mu\text{M}$) was reduced. We also did the real time PCR for NM23 and MMP2. We suggested that FIP-fve increased NM23 mRNA expressions but no effect on MMP2 (Figure 4D).

FIP-fve Regulates Migration of A549 cells via RacGAP1. To clarify the role of RacGAP1 in FIP-fve-mediated lung cancer cell migration and proliferation, RacGAP1 silencing (Figure 5A) experiments were carried out with a VZV-G pseudotyped lentivirus-shRNA system. Cell migration was determined using in vitro wound-healing assay. The migration ability of A549 shLuc cells was similar to that of parental A549 cells, and shRacGAP1-47297 and shRacGAP1-47293 showed slower migration toward the gap area than controls (Figure 5B). Compared with the controls, the shRacGAP1-47297 and shRacGAP1-47293 A549 cells showed 70% and 80% reductions, respectively, at 24 h. At 48 h, the shRacGAP1-47297 and shRacGAP1-47293 A549 cells showed 62% and 76% reductions, respectively (Figure 5C). In addition, we investigated shRacGAP1-47297 and shRacGAP1-47293 that inhibit the cell migration to 48% and 43%, respectively (Figure 5D,E). Furthermore, we investigated the migratory ability under the condition of overexpression of RacGAP1 cells. The RacGAP1 protein showed a 1.54-fold increase in comparison with pLKO-RacGAP1 and pLKO-EGFP in parental cells (Figure 6A). Migrating A549/pLKO-RacGAP1 cells increased (Figure 6B) to 135% and 124% at 24 and 48 h, respectively, when compared with controls (Figure 6C).

DISCUSSION

RacGAP1, also called MgcRacGAP, Cyk4, and ID-GAP, is an evolutionarily conserved GTPase-activating protein (GAP) in the Rho family of GTPases. It has been reported that RacGAP1

controls the mitotic spindle and plays an important role in the completion of cytokinesis, accumulating in the midbody.²⁵ RacGAP1 is one of the genes that have been identified in the prediction of risk of early recurrence. High expression of RacGAP1 is significantly associated with the early recurrence of human hepatocellular carcinoma (HCC).^{22,26} RACGAP1 is also overexpressed in the SPC-A-1, GLC-82, 801D, and EPLC-32M1 lung cancer cell lines when compared with the immortalized human bronchial epithelial cell line BEAS-2B. However, reduced RACGAP1 expression does not affect the rate of cellular proliferation or the number of apoptotic cells in SPC-A-1 and GLC-82 cell lines.²⁷ In this study, we have demonstrated for the first time that FIP-fve significantly inhibits migratory and invasive capabilities of A549 lung cancer cells by decreasing RacGAP1 expression and Rac1 activity (Figure 7). In addition,

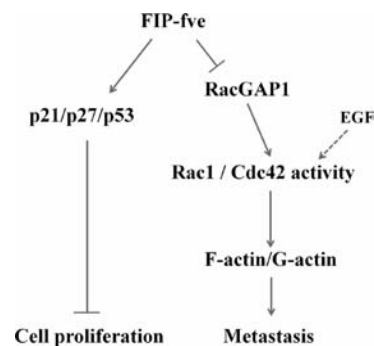


Figure 7. Summary model of inhibition of lung cancer metastasis and proliferation function by FIP-fve. FIP-fve inhibited metastasis and proliferation of A549 cells by decreasing the expression of RACGAP1.

FIP-fve inhibits filopodia fiber formation to interrupt the migratory ability of A549 lung cancer cells. There was reported that GMI inhibited EGF-induced migration and invasion in

A549 cells through blocking PI3K/Akt pathway.²⁸ NM23 suppresses migration of cervical cancer cells and enhances the migration inhibition of FIP-gts.²⁹ It may be suggested that FIP-fve interrupts the A549 cell migration through blocking PI3K/Akt pathway or NM23 increased.

As major cell cycle arrest signals, p53, p21, and E2F1 participate in G1 arrest.³⁰ Tumor suppressor gene p53 is a crucial factor in the induction of cell-cycle arrest and apoptosis following ionizing radiation or DNA damage in human cells.^{31,32} In addition, p53-dependent cell-cycle arrest is involved in transactivation of p21WAF1/Cip1 or other related factors, while p21WAF1/Cip1 is induced in G1 or G2/M arrest of the cell cycle. We demonstrated that FIP-fve results in G₁ arrest through increased P21, P27, and P53 and decreased E2F-1 expressions. Knockdown of CDCA2 with shRNA system significantly inhibited ($P < 0.05$) cellular proliferation when compared with control cells by arresting G1 phase of cell-cycle progression and up-regulating the cyclin-dependent kinase inhibitors (p21(Cip1), p27(Kip1), p15(INK4B), and p16(INK4A)).³³

Our previous study showed that FIP-fve stimulates IFN- γ in PBMCs.¹¹ IFN- γ regulates the trafficking of specific immune cells to sites of inflammation (e.g., tumor sites) through induction of expression of adhesion molecules (e.g., ICAM-1, VCAM-1) and chemokines (e.g., IP-10, MCP-1, MIG-1a/b, RANTES).³⁴ Combined IFN- γ and TNF treatment drives Tag-expressing cancers into senescence by inducing growth arrest in G1/G0 phase, with activation of p16INK4a (also known as CDKN2A) and downstream Rb hypophosphorylation at serine 795.³⁵ In this study, we demonstrated that FIP-fve inhibits lung cancer metastasis and proliferation. The role of IFN- γ production in FIP-fve-induced cell cycle arrest requires further investigation.

Oral administration of FIP-fve generates significant antitumor activity in mice bearing BNL hepatoma cells. Combination treatment of FIP-fve with anti-IFN- γ neutralizes mAb, resulting in lower antitumor effect than with FIP-fve treatment alone.³⁶ Another fungal immunomodulatory protein, Ling Zhi-8 (LZ-8), has 63% protein sequence identity with FIP-fve.³⁷ Recombinant LZ-8 (rLZ-8) inhibits cell growth that is correlated with increased G1 arrest. Moreover, rLZ-8 activates p53 and p21 expressions and both G1 arrest and antiproliferation are induced by ribosomal protein S7-MDM2-p53 dependent pathway.³⁸ LZ-8 has been found to enhance dendritic cell-induced antigen-specific T cell activation in vitro and in a subunit vaccine model in vivo. Co-treatment with LZ-8 as an adjuvant has been shown to dramatically improve the therapeutic efficacy of DNA vaccine against murine bladder (MBT-2) tumor.³⁹ In addition, reFIP-gts has been found to induce cell cycle G1 arrest and senescence in lung cancer cells.⁴⁰ GMI from *Ganoderma microsporium* is yet another fungal immunomodulatory protein. It inhibits metastatic ability regulated by epidermal growth factor (EGF) in A549 cells.⁴¹

In conclusion, our data provide evidence that FIP-fve reduces RacGAP expression resulting in antimetastasis and suppression of the proliferation of A549 cells via p53 activation pathway.

AUTHOR INFORMATION

Corresponding Authors

*For J.-L.K.: phone, (886-4) 24730022-11694; E-mail, jlko@csmu.edu.tw.

*For K.-H.L.: E-mail, cshy095@csh.org.tw.

Funding

This work was supported by grant no. CSH-2012-D-002 from the Chung-Shan Medical University Hospital, Taichung, Taiwan.

Notes

The authors declare no competing financial interest.

ABBREVIATIONS USED

FIP, Fungal immunomodulatory protein; TLRs, Toll-like receptors; IFN- γ , interferon-gamma; hPBMCs, human peripheral blood mononuclear cells; LCN2, lipocalin 2; RacGAP1, Rac GTPase-activating protein 1; PAI-1, plasminogen activator inhibitor type-1; MMP2, matrix metalloproteinase

REFERENCES

- (1) Paez, J. G.; Janne, P. A.; Lee, J. C.; Tracy, S.; Greulich, H.; Gabriel, S.; Herman, P.; Kaye, F. J.; Lindeman, N.; Boggon, T. J.; Naoki, K.; Sasaki, H.; Fujii, Y.; Eck, M. J.; Sellers, W. R.; Johnson, B. E.; Meyerson, M. EGFR mutations in lung cancer: correlation with clinical response to gefitinib therapy. *Science* **2004**, *304* (5676), 1497–1500.
- (2) Lukasik, D.; Wilczek, E.; Wasiutynski, A.; Gornicka, B. Deleted in liver cancer protein family in human malignancies (Review). *Oncol. Lett.* **2011**, *2* (5), 763–768.
- (3) Zhang, J. Y.; Zhang, D.; Wang, E. H. Overexpression of small GTPases directly correlates with expression of delta-catenin and their coexpression predicts a poor clinical outcome in nonsmall cell lung cancer. *Mol. Carcinog.* **2011**, *52* (5), 338–347.
- (4) Duan, L.; Chen, G.; Virmani, S.; Ying, G.; Raja, S. M.; Chung, B. M.; Rainey, M. A.; Dimri, M.; Ortega-Cava, C. F.; Zhao, X.; Clubb, R. J.; Tu, C.; Reddi, A. L.; Naramura, M.; Band, V.; Band, H. Distinct roles for Rho versus Rac/Cdc42 GTPases downstream of Vav2 in regulating mammary epithelial acinar architecture. *J. Biol. Chem.* **2010**, *285* (2), 1555–1568.
- (5) Mizukawa, B.; Wei, J.; Shrestha, M.; Wunderlich, M.; Chou, F. S.; Griesinger, A.; Harris, C. E.; Kumar, A. R.; Zheng, Y.; Williams, D. A.; Mulloy, J. C. Inhibition of Rac GTPase signaling and downstream prosurvival Bcl-2 proteins as combination targeted therapy in MLL-AF9 leukemia. *Blood* **2011**, *118* (19), S235–S245.
- (6) Wang, X.; He, L.; Wu, Y. L.; Hahn, K. M.; Montell, D. J. Light-mediated activation reveals a key role for Rac in collective guidance of cell movement in vivo. *Nature Cell Biol.* **2010**, *12* (6), S91–S97.
- (7) Qian, X.; Durkin, M. E.; Wang, D.; Tripathi, B. K.; Olson, L.; Yang, X. Y.; Vass, W. C.; Popescu, N. C.; Lowy, D. R. Inactivation of the Dcl1 gene cooperates with downregulation of p15INK4b and p16Ink4a, leading to neoplastic transformation and poor prognosis in human cancer. *Cancer Res.* **2012**, *72* (22), S900–S911.
- (8) Ko, J. L.; Hsu, C. I.; Lin, R. H.; Kao, C. L.; Lin, J. Y. A new fungal immunomodulatory protein, FIP-fve isolated from the edible mushroom, *Flammulina velutipes* and its complete amino acid sequence. *Eur. J. Biochem./FEBS* **1995**, *228* (2), 244–249.
- (9) Ko, J. L.; Lin, S. J.; Hsu, C. I.; Kao, C. L.; Lin, J. Y. Molecular cloning and expression of a fungal immunomodulatory protein, FIP-fve, from *Flammulina velutipes*. *J. Formosan Med. Assoc.* **1997**, *96* (7), 517–524.
- (10) Wang, P. H.; Hsu, C. I.; Tang, S. C.; Huang, Y. L.; Lin, J. Y.; Ko, J. L. Fungal immunomodulatory protein from *Flammulina velutipes* induces interferon-gamma production through p38 mitogen-activated protein kinase signaling pathway. *J. Agric. Food Chem.* **2004**, *52* (9), 2721–2725.
- (11) Ou, C. C.; Hsiao, Y. M.; Wu, W. J.; Tasy, G. J.; Ko, J. L.; Lin, M. Y. FIP-fve stimulates interferon-gamma production via modulation of calcium release and PKC-alpha activation. *J. Agric. Food Chem.* **2009**, *57* (22), 11008–11013.
- (12) Marshall, N. A.; Galvin, K. C.; Corcoran, A. M.; Boon, L.; Higgs, R.; Mills, K. H. Immunotherapy with PI3K inhibitor and Toll-like receptor agonist induces IFN-gamma+IL-17+ polyfunctional T cells

that mediate rejection of murine tumors. *Cancer Res.* **2012**, *72* (3), 581–591.

(13) Buneker, C. K.; Yu, R.; Deedigan, L.; Mohr, A.; Zwacka, R. M. IFN-gamma combined with targeting of XIAP leads to increased apoptosis-sensitisation of TRAIL resistant pancreatic carcinoma cells. *Cancer Lett.* **2012**, *316* (2), 168–177.

(14) Hsin, I. L.; Ou, C. C.; Wu, T. C.; Jan, M. S.; Wu, M. F.; Chiu, L. Y.; Lue, K. H.; Ko, J. L. GMI, an immunomodulatory protein from *Ganoderma microsporum*, induces autophagy in non-small cell lung cancer cells. *Autophagy* **2011**, *7* (8), 873–882.

(15) Wu, M. F.; Hsiao, Y. M.; Huang, C. F.; Huang, Y. H.; Yang, W. J.; Chan, H. W.; Chang, J. T.; Ko, J. L. Genetic determinants of pemetrexed responsiveness and nonresponsiveness in non-small cell lung cancer cells. *J. Thorac. Oncol.* **2010**, *5* (8), 1143–1151.

(16) Hsin, I. L.; Hsiao, Y. C.; Wu, M. F.; Jan, M. S.; Tang, S. C.; Lin, Y. W.; Hsu, C. P.; Ko, J. L. Lipocalin 2, a new GADD153 target gene, as an apoptosis inducer of endoplasmic reticulum stress in lung cancer cells. *Toxicol. Appl. Pharmacol.* **2012**, *263* (3), 330–337.

(17) Wang, P. H.; Ko, J. L.; Yang, S. F.; Lin, L. Y. Implication of human nonmetastatic clone 23 Type 1 and its downstream gene lipocalin 2 in metastasis and patient's survival of cancer of uterine cervix. *Int. J. Cancer* **2011**, *129* (10), 2380–2389.

(18) Binker, M. G.; Binker-Cosen, A. A.; Richards, D.; Oliver, B.; Cosen-Binker, L. I. EGF promotes invasion by PANC-1 cells through Rac1/ROS-dependent secretion and activation of MMP-2. *Biochem. Biophys. Res. Commun.* **2009**, *379* (2), 445–450.

(19) Donehower, L. A. Using mice to examine p53 functions in cancer, aging, and longevity. *Cold Spring Harbor Perspect. Biol.* **2009**, *1* (6), a001081.

(20) Ong, C. S.; Zhou, J.; Ong, C. N.; Shen, H. M. Luteolin induces G1 arrest in human nasopharyngeal carcinoma cells via the Akt-GSK-3beta-Cyclin D1 pathway. *Cancer Lett.* **2010**, *298* (2), 167–175.

(21) Vignjevic, D.; Montagnac, G. Reorganisation of the dendritic actin network during cancer cell migration and invasion. *Semin. Cancer Biol.* **2008**, *18* (1), 12–22.

(22) Wang, S. M.; Ooi, L. L.; Hui, K. M. Upregulation of Rac GTPase-activating protein 1 is significantly associated with the early recurrence of human hepatocellular carcinoma. *Clin. Cancer Res.* **2011**, *17* (18), 6040–6051.

(23) Shetty, S.; Velusamy, T.; Shetty, R. S.; Marudamuthu, A. S.; Shetty, S. K.; Florova, G.; Tucker, T.; Koenig, K.; Shetty, P.; Bhandary, Y. P.; Idell, S. Post-transcriptional regulation of plasminogen activator inhibitor type-1 expression in human pleural mesothelial cells. *Am. J. Respir. Cell Mol. Biol.* **2009**, *43* (3), 358–367.

(24) Kumar, P.; Yadav, A.; Patel, S. N.; Islam, M.; Pan, Q.; Merajver, S. D.; Teknos, T. N. Tetrathiomolybdate inhibits head and neck cancer metastasis by decreasing tumor cell motility, invasiveness and by promoting tumor cell anoikis. *Mol. Cancer* **2010**, *9*, 206.

(25) Kawashima, T.; Bao, Y. C.; Minoshima, Y.; Nomura, Y.; Hatori, T.; Hori, T.; Fukagawa, T.; Fukada, T.; Takahashi, N.; Nosaka, T.; Inoue, M.; Sato, T.; Kukimoto-Niino, M.; Shirouzu, M.; Yokoyama, S.; Kitamura, T. A Rac GTPase-activating protein, MgcRacGAP, is a nuclear localizing signal-containing nuclear chaperone in the activation of STAT transcription factors. *Mol. Cell. Biol.* **2009**, *29* (7), 1796–1813.

(26) Wang, S. M.; Ooi, L. L.; Hui, K. M. Identification and validation of a novel gene signature associated with the recurrence of human hepatocellular carcinoma. *Clin. Cancer Res.* **2007**, *13* (21), 6275–6283.

(27) Liang, Y.; Liu, M.; Wang, P.; Ding, X.; Cao, Y. Analysis of 20 genes at chromosome band 12q13: RACGAP1 and MCRS1 overexpression in nonsmall-cell lung cancer. *Genes, Chromosomes Cancer* **2013**, *52* (3), 305–315.

(28) Lin, C.-H.; Sheu, G.-T.; Lin, Y.-W.; Yeh, C.-S.; Huang, Y.-H.; Lai, Y.-C.; Chang, J.-G.; Ko, J.-L. A new immunomodulatory protein from *Ganoderma microsporum* inhibits epidermal growth factor mediated migration A549 lung cancer cells. *Process Biochem.* **2010**, *45*, 1537–1542.

(29) Wang, P. H.; Yang, S. F.; Chen, G. D.; Han, C. P.; Chen, S. C.; Lin, L. Y.; Ko, J. L. Human nonmetastatic clone 23 type 1 gene

suppresses migration of cervical cancer cells and enhances the migration inhibition of fungal immunomodulatory protein from *Ganoderma tsugae*. *Reprod. Sci.* **2007**, *14* (5), 475–485.

(30) Sharma, N.; Timmers, C.; Trikha, P.; Saavedra, H. I.; Obery, A.; Leone, G. Control of the p53-p21CIP1 axis by E2f1, E2f2, and E2f3 is essential for G1/S progression and cellular transformation. *J. Biol. Chem.* **2006**, *281* (47), 36124–36131.

(31) Amaral, J. D.; Xavier, J. M.; Steer, C. J.; Rodrigues, C. M. The role of p53 in apoptosis. *Discovery Med.* **2010**, *9* (45), 145–152.

(32) Petersen, L.; Hasvold, G.; Lukas, J.; Bartek, J.; Syljuasen, R. G. p53-dependent G(1) arrest in 1st or 2nd cell cycle may protect human cancer cells from cell death after treatment with ionizing radiation and Chk1 inhibitors. *Cell Proliferation* **2010**, *43* (4), 365–371.

(33) Uchida, F.; Uzawa, K.; Kasamatsu, A.; Takatori, H.; Sakamoto, Y.; Ogawara, K.; Shiiba, M.; Bukawa, H.; Tanzawa, H. Overexpression of CDCA2 in human squamous cell carcinoma: correlation with prevention of G1 phase arrest and apoptosis. *PLoS One* **2013**, *8* (2), e56381.

(34) Xu, W.; Jones, M.; Liu, B.; Zhu, X.; Johnson, C. B.; Edwards, A. C.; Kong, L.; Jeng, E. K.; Han, K.; Marcus, W. D.; Rubinstein, M. P.; Rhode, P. R.; Wong, H. C. Efficacy and Mechanism-of-Action of a Novel Superagonist Interleukin-15: Interleukin-15 Receptor alphaSu/Fc Fusion Complex in Syngeneic Murine Models of Multiple Myeloma. *Cancer Res.* **2013**, *73*, 3075–3086.

(35) Braumuller, H.; Wieder, T.; Brenner, E.; Assmann, S.; Hahn, M.; Alkhaled, M.; Schilbach, K.; Essmann, F.; Kneilling, M.; Griessinger, C.; Ranta, F.; Ullrich, S.; Mocikat, R.; Braungart, K.; Mehra, T.; Fehrenbacher, B.; Berdel, J.; Niessner, H.; Meier, F.; van den Broek, M.; Haring, H. U.; Handgretinger, R.; Quintanilla-Martinez, L.; Fend, F.; Pesic, M.; Bauer, J.; Zender, L.; Schaller, M.; Schulze-Osthoff, K.; Rocken, M. T-helper-1-cell cytokines drive cancer into senescence. *Nature* **2013**, *494* (7437), 361–365.

(36) Chang, H. H.; Hsieh, K. Y.; Yeh, C. H.; Tu, Y. P.; Sheu, F. Oral administration of an Enoki mushroom protein FVE activates innate and adaptive immunity and induces anti-tumor activity against murine hepatocellular carcinoma. *Int. Immunopharmacol.* **2010**, *10* (2), 239–246.

(37) Liu, Y. F.; Chang, S. H.; Sun, H. L.; Chang, Y. C.; Hsin, I. L.; Lue, K. H.; Ko, J. L. IFN-gamma Induction on Carbohydrate Binding Module of Fungal Immunomodulatory Protein in Human Peripheral Mononuclear Cells. *J. Agric. Food Chem.* **2012**, *60* (19), 4914–4922.

(38) Wu, C. T.; Lin, T. Y.; Hsu, H. Y.; Sheu, F.; Ho, C. M.; Chen, E. I. Ling Zhi-8 mediates p53-dependent growth arrest of lung cancer cells proliferation via the ribosomal protein S7-MDM2-p53 pathway. *Carcinogenesis* **2011**, *32* (12), 1890–1896.

(39) Lin, C. C.; Yu, Y. L.; Shih, C. C.; Liu, K. J.; Ou, K. L.; Hong, L. Z.; Chen, J. D.; Chu, C. L. A novel adjuvant Ling Zhi-8 enhances the efficacy of DNA cancer vaccine by activating dendritic cells. *Cancer Immunol. Immunother.* **2011**, *60* (7), 1019–1027.

(40) Liao, C. H.; Hsiao, Y. M.; Lin, C. H.; Yeh, C. S.; Wang, J. C.; Ni, C. H.; Hsu, C. P.; Ko, J. L. Induction of premature senescence in human lung cancer by fungal immunomodulatory protein from *Ganoderma tsugae*. *Food Chem. Toxicol.* **2008**, *46* (5), 1851–1859.

(41) Lin, C. H.; Hsiao, Y. M.; Ou, C. C.; Lin, Y. W.; Chiu, Y. L.; Lue, K. H.; Chang, J. G.; Ko, J. L. GMI, a *Ganoderma* immunomodulatory protein, down-regulates tumor necrosis factor alpha-induced expression of matrix metalloproteinase 9 via NF-kappaB pathway in human alveolar epithelial A549 cells. *J. Agric. Food Chem.* **2010**, *58* (22), 12014–12021.